



## Supplementary Materials for

### **Loss of avian phylogenetic diversity in neotropical agricultural systems**

Luke O. Frishkoff,\* Daniel S. Karp,\* Leithen K. M’Gonigle, Chase D. Mendenhall, Jim Zook, Claire Kremen, Elizabeth A. Hadly, Gretchen C. Daily

\*Corresponding author. E-mail: [frishkol@stanford.edu](mailto:frishkol@stanford.edu) (L.O.F.), [dkarp@berkeley.edu](mailto:dkarp@berkeley.edu) (D.S.K.)

Published 12 September 2014, *Science* **345**, 1343 (2014)  
DOI: 10.1126/science.1254610

#### **This PDF file includes:**

Materials and Methods  
Figs. S1 to S10  
Tables S1 to S6  
References



## Supplementary Materials for

### **Loss of avian phylogenetic diversity in neotropical agricultural systems**

Luke O. Frishkoff<sup>†</sup>, Daniel S. Karp<sup>†</sup>, Leithen K. M'Gonigle, Chase D. Mendenhall, Jim Zook,  
Claire Kremen, Elizabeth A. Hadly, Gretchen C. Daily

Correspondence to: [gdaily@stanford.edu](mailto:gdaily@stanford.edu)

<sup>†</sup>Authors contributed equally

#### **This PDF file includes:**

Materials and Methods  
Figs. S1 to S10  
Tables S1 to S6

## Materials and Methods

### Bird Censuses

We used a long-term dataset of bird censuses to quantify how habitat conversion and agricultural intensification affect the evolutionary history held within bird communities. We obtained twelve years of survey data (2001-2012), collected in four regions across Costa Rica, each separated by ~200km. The study regions encompassed a variety of life zones and agricultural systems: Guanacaste (tropical dry forest; melon, rice, sugar cane, cattle, and aquaculture), Las Cruces (premontane wet forest; coffee, pasture), Puerto Viejo (lowland wet forest; heart-of-palm, banana, mixed gardens, pasture), and San Isidro (mid-elevation wet forest; coffee, pineapple, sugar cane, pasture) (1). Twelve 200m transects were placed in each study region in three land uses: forest reserves, diversified agriculture, and intensive monocultures. Unlike intensive monocultures, diversified agriculture contained not only a variety of crop species, but also more natural vegetation, including hedgerows and nearby forest patches (Table S1). Four transects were substantially modified throughout the survey period and changed in land-use classification; therefore, we restricted our analyses to 44 transects—12 in forest reserves, 16 in diversified agriculture, and 16 in intensive monocultures.

The same expert ornithologist (J. Zook) conducted all censuses. Each transect was visited six times each year, in two three-visit intervals over approximately one week during the dry (February-May) and wet seasons (September-November). Three transects were visited per day, beginning at sunrise, and the visitation order was varied so that transects were surveyed at multiple times. Censuses involved walking the 200m transect for 30min, recording all visual and auditory bird detections within 50m of either side of the transect line. If time remained after walking the full 200m, then transects were walked in the opposite direction. Multiple individuals of the same species were counted only if they were simultaneously detected or could be visually separated (e.g., by age or sex). Flythrough birds and flyovers were excluded.

### Habitat Affinity

Habitat affinity was calculated by running a hierarchical occupancy model for the 308 species encountered more than 25 times during the transect walks (occupancy modeling procedure described below). Results were robust to including only birds encountered more than 10 and also more than 50 times. The occupancy of a species describes the probability that a species exists in a given habitat during a sampling period, and ranges from 0 to 1. We then calculated a species' habitat affinity by considering its occupancy probability while controlling for its average occupancy across all land-use types in our dataset. For analysis purposes we linearized the occupancy score with a logit transformation. Habitat affinity of species  $i$  in land-use  $j$  was calculated according to:

$$HA_{ij} = \text{logit}(\psi_{ij}) - \text{logit}(\bar{\psi}_i)$$

where  $\psi_{ij}$  denotes the probability of occurrence of species  $i$  in land-use  $j$  and  $\bar{\psi}_i$  denotes the mean probability of occurrence of species  $i$  across all three habitat types. Note that the habitat affinity indices take into account mean occupancy across land-use types, so should be read as relative preference for a land-use over the two other land-uses. As such, for a given species, the three habitat affinity indices are not independent of one another. Positive affinity towards one habitat implies negative affinity towards at least one of the other two habitat types.

### Phylogeny

For all analyses we used 500 of 10,000 trees from Jetz *et al.* (18). Of the 500 trees, 250 were selected from each of two backbone trees, derived from established deep avian relationships. See Jetz *et al.* (18) for further details on phylogeny construction.

### Phylogenetic Signal of Habitat Affinity

Phylogenetic signal is the propensity of evolutionarily related species to share similar values for a trait. We asked whether species' affinity with forest, diversified agriculture, and intensive monoculture showed phylogenetic signal using Blomberg's  $K$  (20). While species could not have evolved directly to use agricultural habitats over avian evolutionary history (because agricultural habitats are less than 10,000 years old), sets of traits could predispose them to thrive in natural open habitats and potentially leave a phylogenetic signal in habitat affinity. For each of the 500 phylogenetic trees,  $K$  was calculated for affinity to each habitat in each season using occupancy standardized habitat affinity (see above). To determine whether the observed  $K$  values differed significantly from either no phylogenetic signal ( $K = 0$ ) or Brownian motion evolution ( $K = 1$ ), we employed 1,000 null model simulations for each tree. To test whether the observed  $K$  value differed from  $K = 0$ , we used random tip shuffles. To test whether the observed  $K$  value differed from  $K = 1$ , we simulated Brownian motion evolution along a given tree using the observed variance in habitat affinity. The  $p$ -value associated with each tree represents the proportion of simulations for which  $K$  was greater (for  $K = 0$ ) or smaller (for  $K = 1$ ) than the observed  $K$ . We report the median  $p$ -value for each test across all trees (Table S2).

We also compared the fit of alternative models of the evolutionary process: (i) a strict Brownian motion model, in which habitat affinity values evolve at a constant rate throughout the tree; (ii) a model based on Pagel's  $\lambda$ , in which evolution along branches is Brownian, but branch lengths of the tree are transformed by a  $\lambda$  parameter to reduce the amount of phylogenetic signal (identical to Brownian motion model when  $\lambda = 1$ ); (iii) an Ornstein-Uhlenbeck model, in which affinities evolve, but tend to be pulled towards a central affinity value with a strength determined by the parameter  $\alpha$ , (identical to Brownian motion model when  $\alpha = 0$ ); and (iv) a white noise model in which phylogenetic relatedness has no impact on values of a trait. All models were calculated on the time-calibrated tree, so units of  $\alpha$  are in million years<sup>-1</sup>. We compared these four models using the median AICs from across the 500 phylogenetic trees (Table S3).

### Family Level Habitat Affinity

We employed randomization tests to identify bird families that showed greater affinity for particular land-use types than expected by chance. We grouped birds according to family following the classification of the American Ornithological Union. The exception was Emberizidae, the sparrows, which were polyphyletic according to the Jetz *et al.* (18) phylogenies. This group was split into a 'seedeater' clade containing seedeaters in the genera *Oryzoborus*, *Sporophila*, and *Chlorospingus* and grassquits in the genus *Tiaris* and *Volatinia*, as well as a 'sparrow' clade containing the genera *Arremon*, *Arremonops*, *Zonotrichia*, and *Peucaea*. To assess which families were more closely affiliated with specific habitats, the mean habitat affinity for the family was compared to the means of 10,000 draws of the same number of species from a random pool of all species with calculated habitat affinities. Families whose mean affinity was greater than 95% of these draws were considered significantly affiliated with that habitat (Table S4).

### Community Composition and Nestedness

We tested whether transects from different land-use types were nested subsets of one another using the NODF metric, which assess nestedness through species overlap and decreasing fill. The metric spans from 0 (no nestedness) to 100 (complete nestedness). We calculated NODF for each pair of transects within a region. In all cases NODF was very low (Mean 4.1, SD: 2.2) indicating that nestedness between transects is not a defining pattern in this system. The low degree of nesting (especially between forest and agricultural transects) is visually apparent in Fig. S4.

### Phylogenetic Diversity Metrics

Phylogenetic Diversity (PD), was calculated as the total branch length of all species observed at a transect during the six visits in a given year. We explored whether local species richness drove patterns in PD through two methods. First, we calculated the expected phylogenetic diversity of each transect in each year given observed species richness using the ‘expected.pd’ function in the R package ‘picante’. We then calculated the percent deviation of observed phylogenetic diversity from expected phylogenetic diversity (Fig S2a). Second, using each transect in each year as a replicate, we regressed observed species richness against phylogenetic diversity, and extracted the residuals for analysis (Fig S2b).

To determine whether communities in specific land-use types were more or less closely related to one another than expected, we calculated the Mean Phylogenetic Distance (MPD) and Mean Nearest Taxon Distance (MNTD) (29) for each transect in each year. These metrics measure the average number of years of evolutionary history separating all species in a community (MPD) and the average number of years separating each species from its closest relative in the community (MNTD). The number of species in a community and the structure of the phylogeny of the regional species pool can influence both metrics. To remove effects of species richness and regional phylogenetic structure, we compared observed MPD and MNTD against metrics calculated from null communities.

First, we generated null communities by randomly drawing the same number of species as observed on each transect from a species pool. We used four different species pools: (i) global: null communities for a transect were assembled drawing species from all species observed in the study; (ii) land-use: communities were generated drawing only from species that were found in the transect’s land-use type; (iii) region: species were drawn from all species encountered in the study region of a transect; and (iv) land-use  $\times$  region: species were drawn only from the species pool from within the same region and land-use type of the focal transect. Null communities were assembled by randomly drawing  $N$  species from the pool, where  $N$  was the number of species observed at a given transect during a given year. The probability of drawing a species was proportional to the frequency that the species occurred within transects that defined the species pool.

Next, we calculated MPD and MNTD for all 1000 null communities for each transect in each year. We then compared observed MPD/MNTD to the distributions of MPD/MNTD calculated from null communities, and extracted the centile of the observed MPD/MNTD. For example, if observed MPD was greater than 90% of null MPDs, then the transect received a centile value of 0.90. The resulting centile index indicates phylogenetic clustering when values are close to 0, and phylogenetic over-dispersion when values are close to 1. The process was completed for all 500 phylogenies, and the mean MPD/MNTD centiles across phylogenies of each transect-year combination were retained for further analysis.

### Evolutionary Distinctness and Diversification

We quantified the evolutionary distinctness of each species using the Fair Proportion metric, now available for all birds globally (17). Species with few relatives and branches deep in the tree have high distinctness values, while species with many close relatives have low values. To assess how average diversification rate varied between land-use types, we used two methods. First, we calculated the diversification rate (DR) of each species (18) defined as the inverse of the equal splits metric of evolutionary distinctness. While DR and fair proportion ED are distinct metrics, they are strongly negatively correlated, as rapidly diversifying species have many close relatives, and therefore low ED. Second, we calculated the number of diversification events (splits in the phylogenetic tree) that each species had experienced in the last 1 to 10 million years before present. We calculated DR and number of diversification events for each of the 500 phylogenies of 9,993 species, and took the median value to represent the best estimate of the true value for a species. Finally, we calculated the average evolutionary distinctness or diversification rate/events for all species encountered within a transect for each year for analysis.

### Agriculture Affinity, Diversification Rate, and Natural Open Habitats

We also tested whether diversification rate was positively correlated with species' habitat preferences, by regressing habitat affinity scores against species DR using phylogenetic generalized least squares (PGLS). PGLS models covariance in trait values between pairs of species according to different phylogenetic hypotheses. For each of the 500 trees we tested covariance structures based on (i) Brownian motion evolution, (ii) Pagel's  $\lambda$ , in which the expected covariance based on Brownian motion is multiplied by parameter  $\lambda$  (estimated from the data), and (iii) white noise evolution, in which phylogenetic relatedness does not predict trait covariance. We selected the best-fit model based on comparing candidate median model AIC from across the 500 trees. For all habitat affiliation indices, the covariance structure defined by Pagel's  $\lambda$  outperformed both the covariance structure defined by white noise evolution (mean  $\Delta$ AIC across habitat indices [range]: 25.8 [18.5-35.6]), and strict Brownian motion evolution (mean  $\Delta$ AIC across habitat indices [range]: 156.6 [135.2-204.9]). We present only slopes and significance from the models using the  $\lambda$  covariance structure (Table S6), though slopes are qualitatively similar regardless of the covariance structure used.

Similarly, we assessed whether natural open habitat specialists were preadapted to exploit agriculture by testing whether use of specific natural open habitats was associated with higher or lower scores on the habitat affinity indices for forest, diversified agriculture, and intensive monocultures. We obtained species presence or absence from natural open habitats from (30). Again using a PGLS framework, we tested Brownian motion, Pagel's  $\lambda$ , and white noise covariance structures to take into account phylogenetic relatedness. For all habitat affiliation indices, and all natural open habitat types, the covariance structure defined by Pagel's  $\lambda$  outperformed both the covariance structure defined by white noise evolution (mean  $\Delta$ AIC across habitat indices and open habitat types [range]: 24.7 [15.8-35.5]), and strict Brownian motion evolution (mean  $\Delta$ AIC across habitat indices and open habitat types [range]: 174.9 [140.1-229.0]).

Finally, we used PGLS to test whether open habitat species had higher diversification rates (DR) than birds not associated with natural open habitats. A covariance matrix defined by Pagel's  $\lambda$  again consistently outperformed other covariance structures (Pagel's  $\lambda$  versus white noise evolution, mean  $\Delta$ AIC across open habitat types [range]: 45.7 [42.3-48.7], Pagel's  $\lambda$  versus Brownian motion evolution: mean  $\Delta$ AIC across open habitat types [range]: 27.8 [18.2-31.8]).

## Statistical Analysis

We tested alternative models of phylogenetic signal in habitat affinity using the `fitContinuous` function in the ‘`geiger`’ package in R. We implemented Generalized Linear Mixed Models to quantify changes in bird diversity metrics across our land-use gradient. For count data (i.e. species richness and median diversifications over the last 1-10 million years), we used Poisson error structures and log links. For continuous data (i.e. phylogenetic diversity, MPD, and MNTD), we implemented Gaussian errors and identity links. In all cases, land-use type was the only fixed effect. Because diversity metrics were calculated for each transect and year, we also included dates (survey year) and locations (transects nested within study regions) as random effects. We then iteratively dropped individual random effects and then the fixed effect to arrive at the most parsimonious model through comparing nested models with AIC and likelihood ratio tests. Mixed effect models were instituted using the R package ‘`lme4`’. Community phylogenetic analyses were conducted using the ‘`Picante`’ and ‘`ape`’ packages in R. PGLS models were conducted using the ‘`ape`’ and ‘`nlme`’ packages. To obtain p-values from PGLS models we used likelihood ratio tests, comparing models with the optimal phylogenetic covariance structure, with and without the fixed effect of interest.

## Occupancy Modeling

We employed a hierarchical framework that explicitly incorporates uncertainty in the detection process into estimation of occupancy parameters (31). Because our goal was to draw conclusions about bird communities, rather than about individual species, we used a model that links occurrence data from multiple species by creating community-level distributions from which species-specific parameter estimates were then drawn (22, 31).

In order to estimate occupancy parameters, we chose to model only the 308 species that had been encountered more than 25 times over the course of the 12 year dataset. Including species that have been encountered fewer times can lead to numerical problems and false convergence in the model. Further, true occupancies in each of our three land-use types would be difficult to calculate for these rarely encountered species. Despite this, we also attempted running the model dropping 0, 10, and 50 species instead of 25. Doing so did not qualitatively change any of our conclusions.

Specifically, we developed a hierarchical multi-season multi-species model in order to estimate occupancy dynamics. We let  $z_{i,j,t}$  denote the true occupancy state of species  $i$  in year  $t$  at site  $j$ . We then let  $x_{i,j,t,k}$  indicate whether we detected ( $x_{i,j,t,k} = 1$ ) or did not detect ( $x_{i,j,t,k} = 0$ ) that species in the  $k^{\text{th}}$  visit to site  $j$  in year  $t$ . We assumed that the occupancy of species  $i$  at site  $j$  in year  $t$  is a Bernoulli random variable  $z_{i,j,t} \sim \text{Bern}(\psi_{i,j,t})$  with probability  $\psi_{i,j,t}$ . In our model, occupancy was the net outcome of a species’ ability to persist in an already occupied site and its ability to colonize vacant sites. Thus, we investigated the effects of our variables of interest on the rates of persistence and colonization, rather than on occupancy directly (described in more detail below). Not all of the bird species occur in each of the four eco-regions. We do not estimate colonization and extirpation rates for species in eco-regions in which they have never been observed.

We first assumed that the occupancy of species  $i$  in site  $j$  in year 1 was given by

$$\psi_{i,j,1} \sim \text{uniform}((0, 1)).$$

unless that site occurs in an eco-region in which species  $i$  does not occur, in which case we set occupancy in year 1 to zero.

We then let  $\varphi_{i,j,t}$  denote the probability that species  $i$  persisted at site  $j$  from years  $t$  to  $t + 1$  (provided it is present at site  $j$  in year  $t$ ) and, similarly, we let  $\gamma_{i,j,t}$  denote the probability that species  $i$  colonized site  $j$  in year  $t + 1$  (provided it is not present at site  $j$  in year  $t$  and that site  $j$  is in a region in which species  $i$  occurs). The probability of occupancy for species  $i$  at site  $j$  could then be computed for each subsequent year as

$$\text{logit}(\psi_{i,j,t+1}) = \varphi_{i,j,t} * z_{i,j,t} + \gamma_{i,j,t} * (1 - z_{i,j,t}),$$

where  $z_{i,j,t} = 1$  if species  $i$  was present in site  $j$  during year  $t$  and 0 if it was not.

In order to quantify the effects of land-use intensity, we defined species-specific persistence and colonization models that included the necessary covariates. Namely, we assumed that between-year persistence was given by

$$\varphi_{i,j,t} = \varphi_{0,i,t} + \varphi_{1,\text{intensity}[j]} + \varphi_{2,\text{region}[j]} + \varphi_{3,\text{intensity}[j]} * \text{evol. distinctness}[i],$$

where  $\varphi_{0,i,t}$  denotes a species-specific effect whose mean across all species varies randomly by year,  $\varphi_{1,\text{intensity}[j]}$  denotes the effect of land use,  $\varphi_{2,\text{region}[j]}$  denotes the effect of region, and  $\varphi_{3,\text{intensity}[j]}$  denotes the effect of evolutionary distinctness within either forest, diversified agriculture, or intensive monocultures. Similarly, the probability of colonization was given by

$$\gamma_{i,j,t} = \gamma_{0,i,t} + \gamma_{1,\text{intensity}[j]} + \gamma_{2,\text{region}[j]} + \gamma_{3,\text{intensity}[j]} * \text{evol. distinctness}[i],$$

where the  $\gamma$  terms are analogous to those for persistence.

Detection was also assumed to be a Bernoulli random variable such that  $x_{i,j,t,k} \sim \text{Bern}(p_{i,j,t,k} * z_{i,j,t})$ , where  $p_{i,j,t,k}$  was the probability that species  $i$  was detected at site  $j$  in the  $k^{\text{th}}$  sample period of the  $t^{\text{th}}$  year, given that it was present. When species  $i$  was absent,  $z_{i,j,t} = 0$ , and thus the detection probability was 0. We allowed detection probabilities to vary by species such that the detection probability of species  $i$  at site  $j$  in the  $k^{\text{th}}$  replicate of the  $t^{\text{th}}$  year was given by

$$\text{logit}(p_{i,j,t,k}) = p_{0,i},$$

where  $p_{0,i}$  was a species-specific affect. We also considered more complex models for detectability (e.g., included region and intensity-specific terms), however, these more complex models were not supported.

As mentioned above, we used a hierarchical community model that links species-specific parameter estimates together by assuming they come from a common distribution. More specifically, the values for  $\varphi_{0,i,t}$ ,  $\gamma_{0,i,t}$ , and  $p_{0,i,t}$  were all drawn from common distributions whose defining parameters were also estimated. We analyzed the model in a Bayesian framework using uninformative priors throughout. For presentation we convert species specific interannual persistence rate ( $\varphi_{i,j}$ ) to a species specific interannual extirpation rate



$(1 - \phi_{i,j})$ .

Occupancy modeling to generate habitat affinity scores was conducted as above, except the terms containing evolutionary distinctness were excluded. We did this to ensure that our calculations of phylogenetic signal were not influenced by habitat affinity indices that already contained phylogenetic information.

#### Trait analysis

Occupancy models for species traits that might predispose species to experience greater extirpation or colonization rates in agriculture were conducted as above, replacing evolutionary distinctness with the trait of interest. We analyzed the following traits, obtained from ((30)), that are thought to regulate bird responses to environmental disturbances (28): body size, clutch size, diet, and diet breadth.

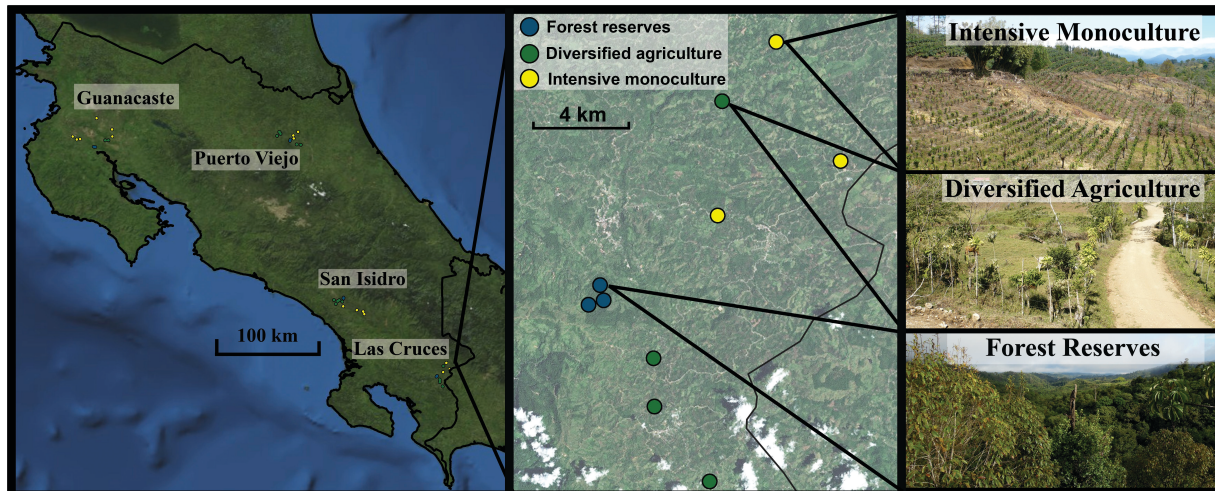


**Fig. S1.**

Map of study sites. Left panel depicts survey transects (colored points) in four study regions (Guanacaste, Puerto Viejo, San Isidro, and Las Cruces). Middle panel shows distribution of survey transects in one study region (Las Cruces). Points are colored according to the land use (blue = forest reserves; green = diversified agriculture; yellow = intensive monocultures). Right panels show photos from transects of each land use.

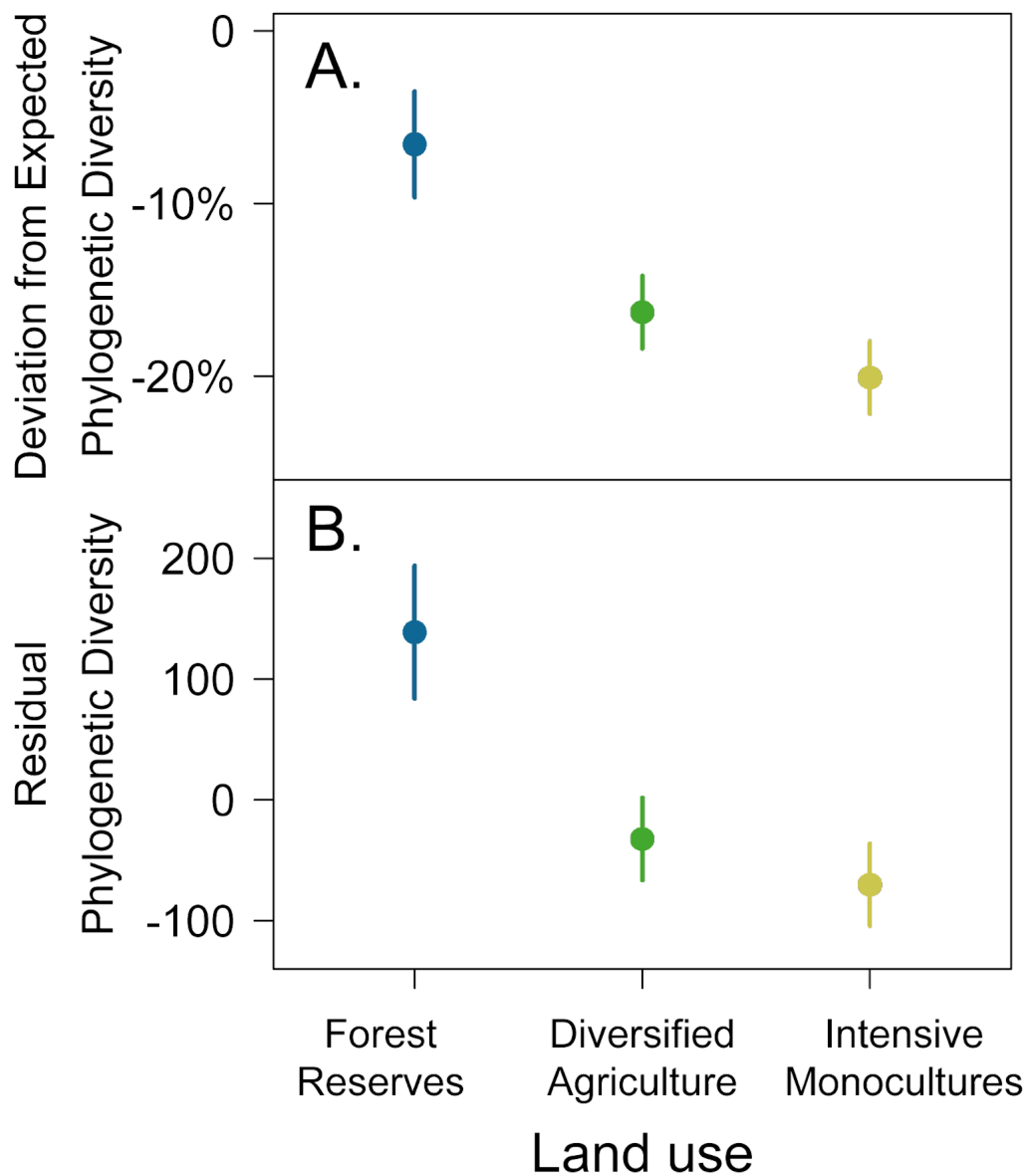


**Fig. S2**

Effect of land use on phylogenetic diversity (PD), after accounting for differences in species richness. Phylogenetic diversity is highest in forest reserves and lowest in intensive monocultures. Panel (A) depicts the percent difference between observed and expected PD, given local species richness and the typology of the bird phylogenetic tree (see Supplementary Methods). Panel (B) depicts differences in residual phylogenetic diversity between land use treatments, after accounting for differences in species richness with linear regression (see Supplementary Methods). Points are predicted means  $\pm$  SEM from generalized linear mixed models (Table S5).  $N_{\text{total}} = 528$  ( $N_{\text{transects}} = 44$ ,  $N_{\text{years}} = 12$ ).

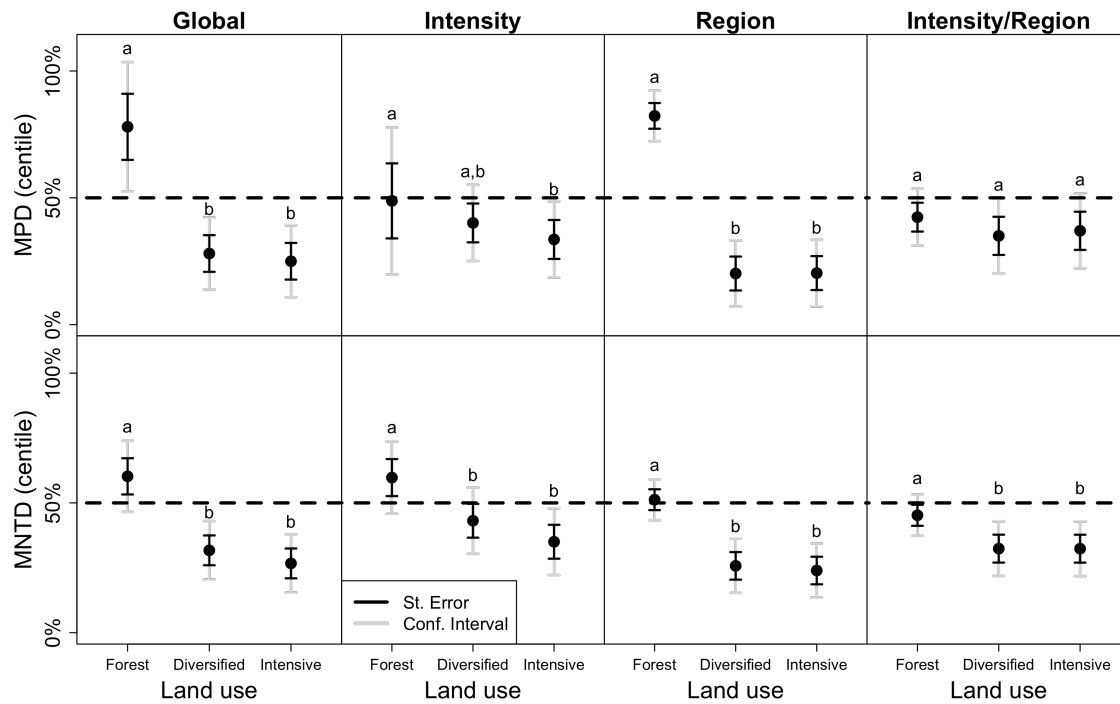


**Fig. S3**

Effect of land use (forest reserves, diversified agriculture, and intensive monocultures) on Mean Phylogenetic Distance (MPD) and Mean Nearest Taxon Distance (MNTD). Points represent mean ( $\pm$  SEM black,  $\pm$  95% CI grey) observed MPD and MNTD centiles within null communities (See Supplementary Methods). Columns correspond to four ways of generating null communities for each transect— the potential species pool was either all surveyed species in Costa Rica (global) or limited to the species that occurred in the same land use, region, or both. In the main text we present MPD using ‘Region’ as the species pool. Values above 50% are indicative of phylogenetic over-dispersion, whereas values below 50% are indicative of clustering. Land uses with different letters (a vs. b) are significantly different (Likelihood Ratio Test:  $P < 0.05$ ).  $N_{\text{total}} = 528$  ( $N_{\text{transects}} = 44$ ,  $N_{\text{years}} = 12$ ).

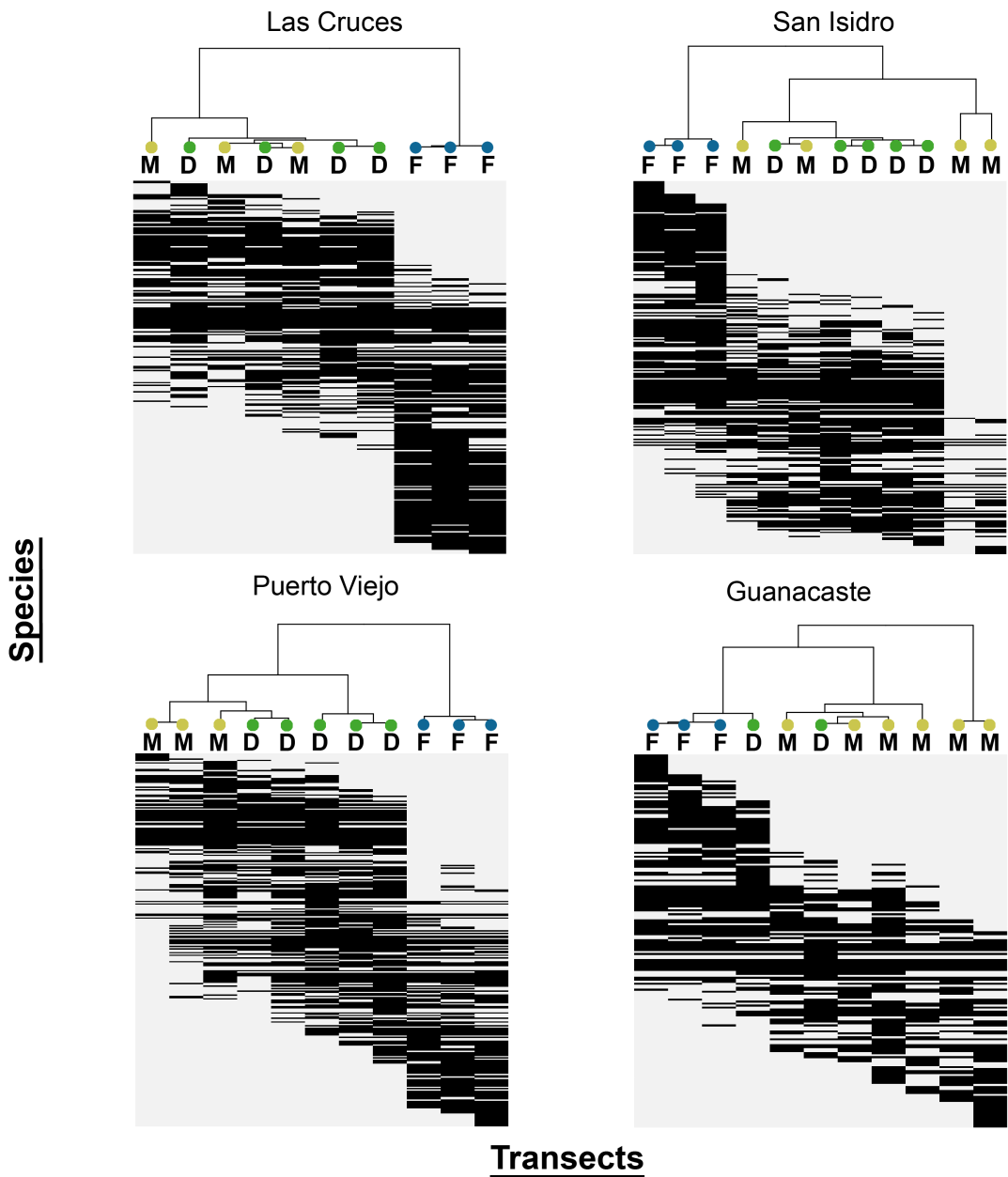


**Fig. S4**

Forest and agriculture possess distinct bird communities, with little nesting. Diagrams depict species presence within each transect in the four study regions. Dendrograms group transects by species similarity, using the Chao community dissimilarity metric. Dots at the tips of dendrograms correspond to transect land uses. Species order and identity in the rows are different for each region, and species that are absent in a region are not shown (*i.e.* row 1 in Las Cruces is not the same species as row 1 in San Isidro).  $N_{\text{transects}} = 44$ ,  $N_{\text{TotalSpp}} = 492$ .

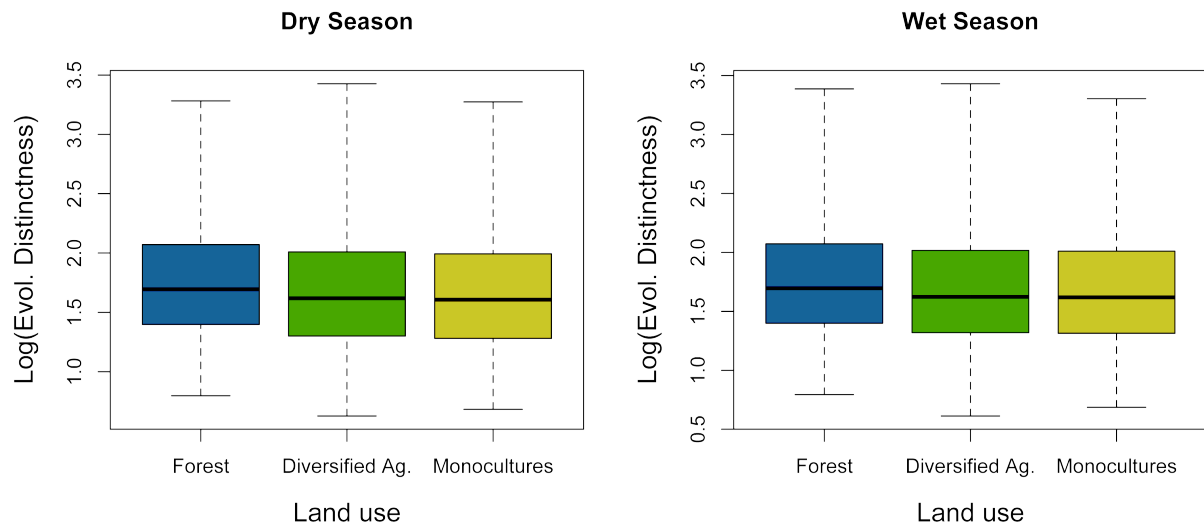


**Fig. S5:** Distributions of evolutionary distinctness scores, weighted by the occupancy rates of each species in each habitat type across all regions. Boxplots demonstrate that, while the difference in mean ED scores between habitat types is significant (Fig. 2D), the effect is small in comparison to the full range of ED scores of birds present across all regions and years.  $N_{\text{spp}} = 308$ .

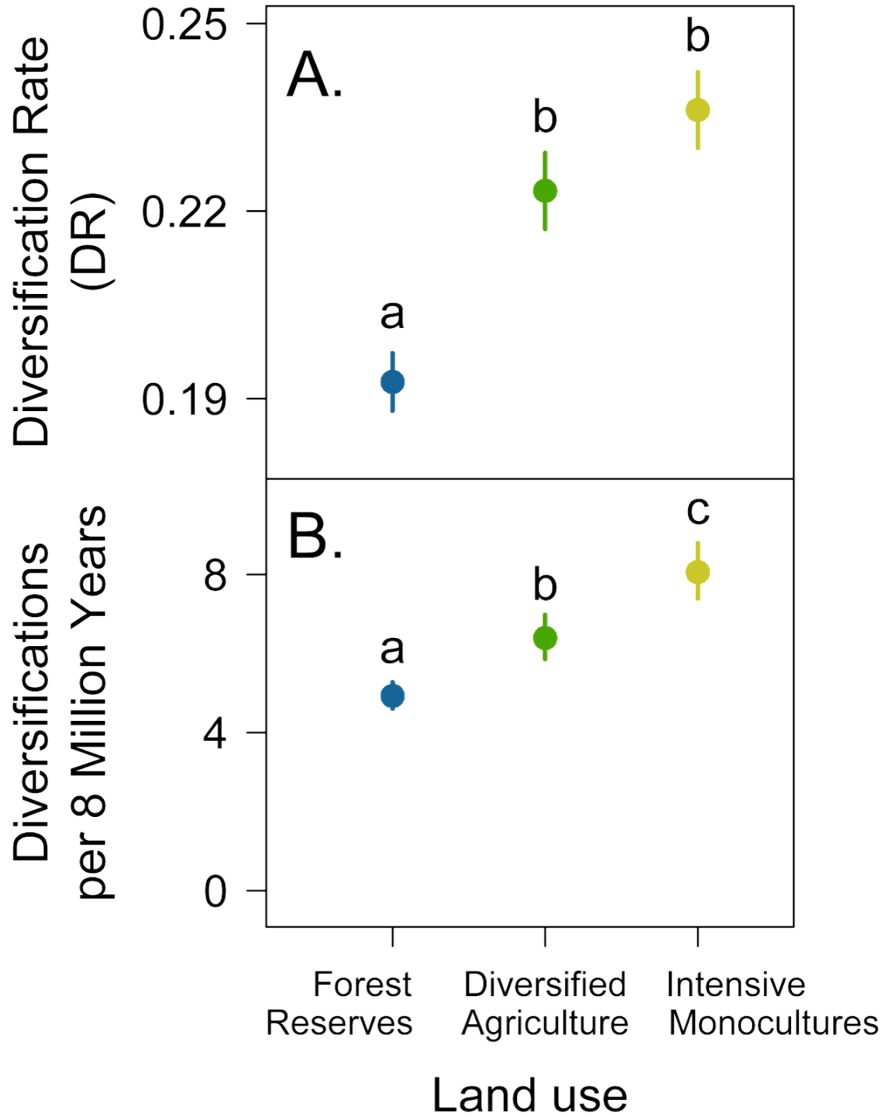


**Fig. S6**

Agricultural intensification favors species that have undergone more diversification events in the recent evolutionary past. Panel (A) depicts differences in the average diversification rates (DR) of species within a transect across land uses. Panel (B) depicts the number of diversification events in a species' clade over the last 8 million years, for the median species in a transect. Results are qualitatively similar across all time frames investigated (from 1-10 million years ago). Points depict predicted mean  $\pm$  SEM from generalized linear mixed models. Different letters denote significant differences between groups (Likelihood Ratio Test:  $P < 0.05$ ).  $N_{\text{total}} = 528$  ( $N_{\text{transects}} = 44$ ,  $N_{\text{years}} = 12$ ).

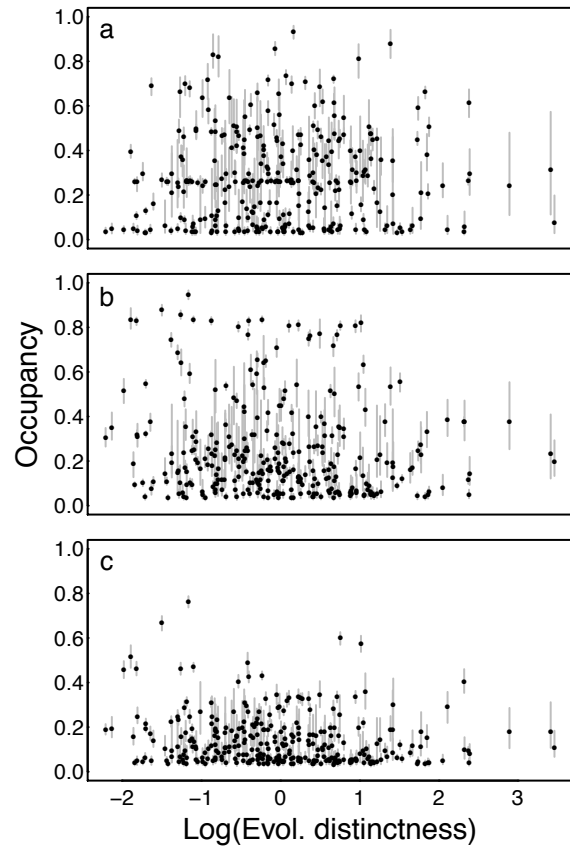


**Fig. S7**

Meta-population occupancy estimates as a function of species' evolutionary distinctness in forest reserves (A), diversified agriculture (B), and intensive monocultures (C). Points are predicted mean  $\pm$  95% BCI of each species.  $N_{\text{spp}} = 308$ ,  $N_{\text{transects}} = 44$ ,  $N_{\text{years}} = 12$ ,  $N_{\text{visits/season}} = 3$ .



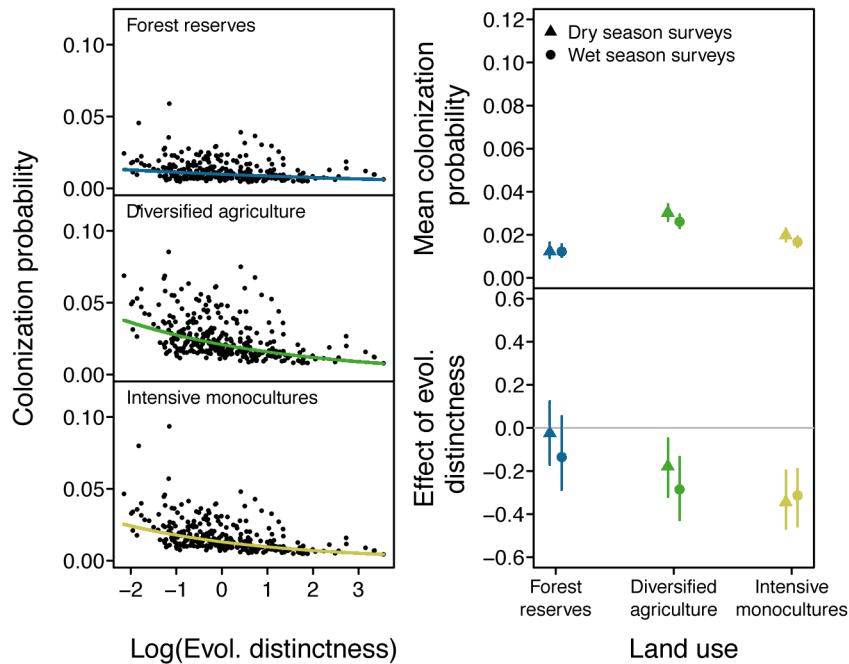


**Fig. S8**

Evolutionarily distinct species exhibit lower between-year colonization rates than less distinct species in intensive monocultures. Between-year probability of colonization (i.e., probability a species is found at a site in one year when not present the previous year) is estimated for each species in each of the three land-use treatments. Panels in (A) show species-specific colonization rates as a function of evolutionary distinctness (standardized, and on a log scale) from wet season surveys in each of the three habitat types. Panel (B) shows average colonization rate across species (means from the left panels) for both seasons. Panel (C) shows the effect of distinctness on extirpation probability (slopes from left panels). For both right panels, points depict mean  $\pm$  95% BCI.  $N_{\text{spp}} = 308$ ,  $N_{\text{transects}} = 44$ ,  $N_{\text{years}} = 12$ ,  $N_{\text{visits/season}} = 3$ .

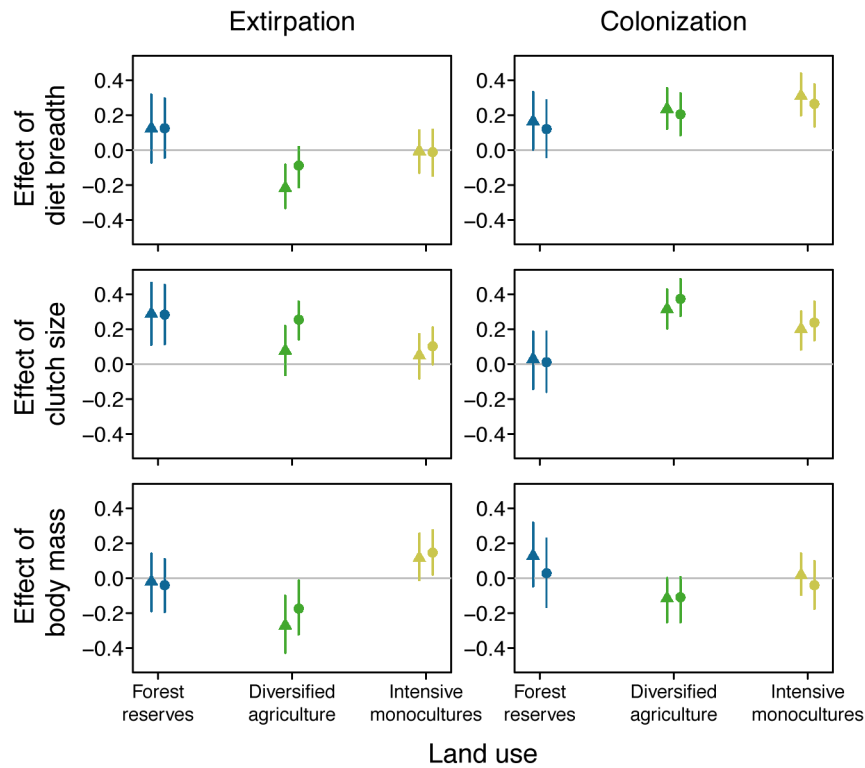


**Fig. S9**

Effects of species traits (diet breadth, clutch size, and body mass) on extirpation and colonization rates in each land use. Left panels depict between-year probability of extirpation (i.e., probability a species is found at a site in one year but not the next year) for each species in each of the three land-use treatments. Right panels depict between-year probability of colonization (i.e., probability a species is found at a site in one year when not present the previous year) for each species in each of the three land-use treatments. Points depict mean  $\pm$  95% BCI.  $N_{\text{transects}} = 44$ ,  $N_{\text{years}} = 12$ ,  $N_{\text{visits/season}} = 3$ ,  $N_{\text{spp diet breadth}} = 290$ ,  $N_{\text{spp clutch size}} = 265$ ,  $N_{\text{spp body mass}} = 305$ .

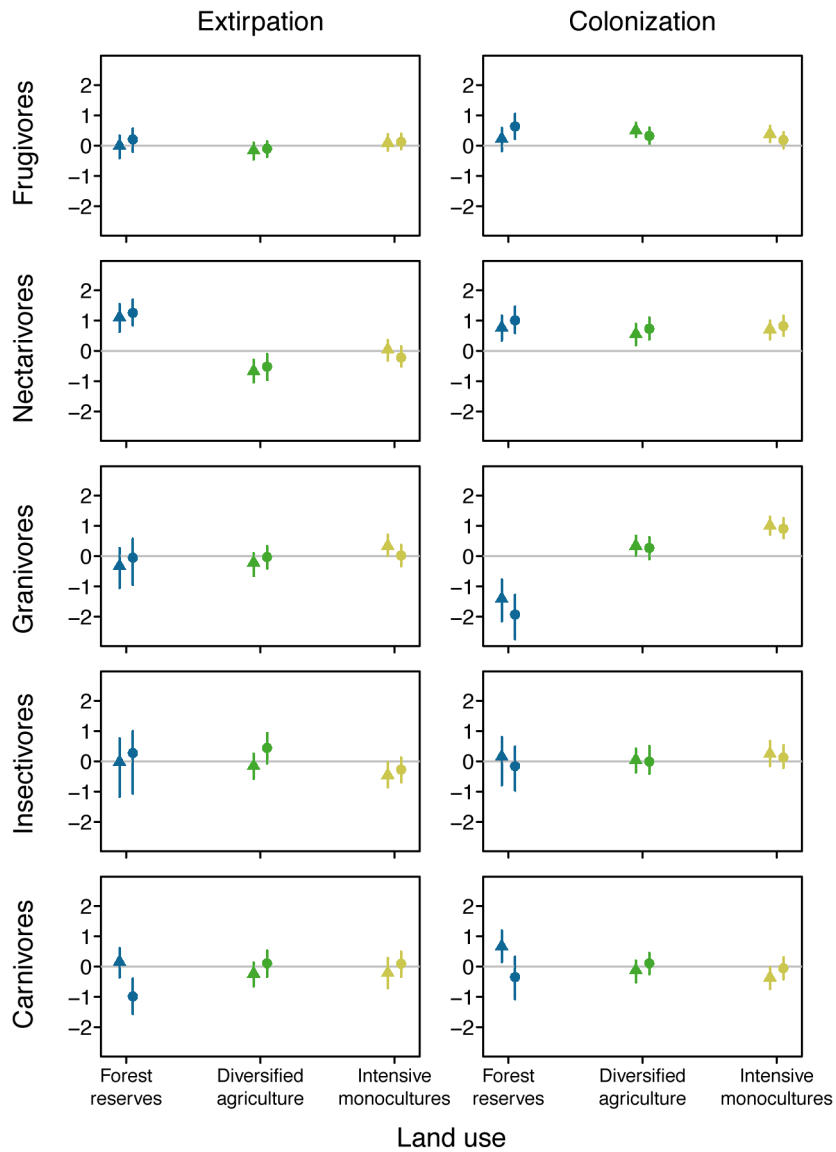


**Fig. S10**

Effect of diet preferences on extirpation (left panels) and colonization (right panels) rates in each of the three land use treatments. Points depict mean extirpation/colonization rates for all species belonging to a given diet guild (e.g. frugivores). Vertical lines are +/- 95% BCI.  $N_{\text{spp}} = 290$ ,  $N_{\text{transects}} = 44$ ,  $N_{\text{years}} = 12$ ,  $N_{\text{visits/season}} = 3$ .

**Table S1:** Structural differences between diversified agriculture and intensive monocultures. Values are means (SD) across transects from surveys conducted in 1999. Table adapted from (1).

	<b>Vegetation Variable</b>	<b>Diversified Agriculture</b>	<b>Intensive Monocultures</b>
<b>Crop Diversity</b>	Number of planted crop species	21.4 (12.8)	4.5 (2.9)
<b>Hedgerow Quality and Extent</b>	% without hedgerows	48.5 (26.6)	69.7 (35.1)
	% short & thin hedgerows	6.2 (5.6)	5.5 (12.1)
	% short & full hedgerows	7.5 (10.3)	9.2 (24.8)
	% tall & thin hedgerows	26.6 (19)	11.6 (18.5)
	% tall & full hedgerows	11.2 (12.4)	3.7 (6.8)
<b>Agricultural plot structure</b>	Plot size (hectares)	3.3 (7.6)	65.5 (78.7)
	Number of bordering plots	6.3 (3.9)	1.9 (1.1)
<b>Forest cover</b>	Proportion tree cover at 100m buffer	0.07 (0.21)	0.01 (0.04)
	Proportion tree cover at 200m buffer	0.10 (0.21)	0.02 (0.06)

**Table S2:** Phylogenetic signal (Blomberg's K) calculations of habitat affinities for all three land-use types in wet and dry seasons. The K metric describes the degree to which a trait adheres to Brownian motion evolution, with values less than 1 indicating a trait is more evolutionarily labile than the Brownian expectation, and values greater than 1 indicating that it is more phylogenetically conserved. When there is no phylogenetic signal (*i.e.* no correlation between phylogeny and values of a trait) K should equal 0. In practice tree topology influences null expectations of K, so significance tests are conducted through randomization tests. Numbers in boxes represents the median value calculated over 500 trees, with the standard deviations in parentheses.  $K_0Null$  is the median K value when habitat affinities are randomly shuffled between tips 1,000 times, and represents the expected K value if there were no phylogenetic signal in the data.  $K_1Null$  is the median K value obtained by simulating Brownian motion evolution of habitat affinity along the tree 1,000 times. P values represent the median number of simulations per tree that were above ( $P_{K=0}$ ) or below ( $P_{K=1}$ ) the observed K value.

		<b>K</b>	<b><math>P_{K=0}</math></b>	<b><math>K_0Null</math></b>	<b><math>P_{K=1}</math></b>	<b><math>K_1Null</math></b>
<b>Forest</b>	Dry	0.15 (0.03)	0.001	0.09 (0.01)	<0.001	0.87 (0.02)
	Wet	0.14 (0.02)	0.002	0.09 (0.01)	<0.001	0.87 (0.02)
<b>Diversified Agriculture</b>	Dry	0.14 (0.02)	0.001	0.09 (0.01)	<0.001	0.87 (0.02)
	Wet	0.12 (0.02)	0.018	0.09 (0.01)	<0.001	0.87 (0.02)
<b>Intensive Monocultures</b>	Dry	0.12 (0.02)	0.010	0.09 (0.01)	<0.001	0.87 (0.02)
	Wet	0.11 (0.02)	0.089	0.09 (0.01)	<0.001	0.87 (0.02)

**Table S3:** Evolutionary models comparison explaining phylogenetic relationships in habitat affinity. Models include strict Brownian motion (BM) evolution, evolution under Brownian motion with species covariances transformed by Pagel’s  $\lambda$  parameter (Lambda), evolution through an Ornstein–Uhlenbeck process (OU), and with no phylogenetic signal (white noise; WN). Alpha values describe the estimated returning power towards the central habitat affinity value in the OU model. Values represent medians across 500 trees, with standard deviations across trees in parentheses.

		<b>BM</b>	<b>Lambda</b>		<b>OU</b>		<b>WN</b>
		<b>AIC</b>	$\lambda$	<b>AIC</b>	<b>Alpha</b>	<b>AIC</b>	<b>AIC</b>
<b>Forest</b>	Dry	1415. (84.0)	0.48 (0.03)	1289.1 (1.5)	0.10 (0.63)	1298.3 (12.2)	1322.3 (0)
	Wet	1405.3 (81.8)	0.39 (0.02)	1273.1 (1.2)	0.11 (0.65)	1281.6 (10.0)	1300.7 (0)
<b>Diversified Agriculture</b>	Dry	1100.8 (81.5)	0.37 (0.02)	962.7 (1.5)	0.11 (0.57)	972.6 (9.3)	988.2 (0)
	Wet	1106.6 (77.7)	0.25 (0.02)	937.9 (0.9)	0.20 (0.58)	949.5 (5.8)	954.3 (0)
<b>Intensive Monocultures</b>	Dry	1061.1 (75.2)	0.45 (0.03)	907.3 (1.2)	0.14 (0.87)	916.9 (10.1)	931.2 (0)
	Wet	1136.4 (77.6)	0.34 (0.03)	940.4 (0.9)	0.22 (1.04)	958.1 (5.4)	958.5 (0)

**Table S4:** Family level habitat affinities for all families that were significantly associated with one land-use type for at least one season. For each family, the mean habitat affinity for a season (Habitat Affinity) was calculated along with the mean habitat affinity that one would expect if drawing the same number of species randomly from the pool of all species. P values denote the proportion of random draws for which the mean habitat affinity was greater than the observed habitat affinity. The family Emberizidae was polyphyletic according to the phylogenies so was split into a ‘Seedeater’ clade and a ‘Sparrow’ clade.

Land Use	English Family	Latin Family	# of Species	Dry Season			Wet Season		
				Habitat Affinity	Null Value	P	Habitat Affinity	Null Value	P
Forest Reserves	Cotingas	Cotingidae	2	2.97	0.65	0.05	1.91	0.60	0.206
	Ovenbirds	Furnariidae	15	1.75	0.65	0.013	1.75	0.60	0.011
	Manakins	Pipridae	6	1.97	0.65	0.051	2.42	0.60	0.013
	Antbirds	Thamnophilidae	14	2.73	0.65	0.001	2.74	0.60	0.001
	Trogons	Trogonidae	5	2.28	0.65	0.028	2.64	0.60	0.011
Diversified Agriculture	Pigeons	Columbidae	13	0.81	0.16	0.015	0.73	0.21	0.054
	Seedeaters	Emberizidae	6	1.55	0.16	0.007	1.48	0.21	0.003
	Blackbirds	Icteridae	14	0.58	0.16	0.078	0.96	0.21	0.007
Intensive Monocultures	Hérons	Ardeidae	2	0.67	-0.81	0.043	0.51	-0.83	0.046
	Pigeons	Columbidae	13	-0.01	-0.82	0.013	-0.25	-0.82	0.029
	Nightjars	Caprimulgidae	1	1.31	0.82	0.039	1.04	-0.82	0.040
	Seedeaters	Emberizidae	6	0.44	-0.81	0.006	0.54	-0.82	0.001
	Estrildid Finches	Estrildidae	1	2.03	-0.83	0.016	0.87	-0.82	0.071
	Swallows	Hirundinidae	4	0.16	-0.82	0.053	0.27	-0.81	0.024
	Blackbirds	Icteridae	14	-0.14	-0.82	0.015	-0.16	-0.82	0.011

**Table S5:** Model comparisons of effect of land use on diversity metrics. Error structures and link functions for each model are reported. Potential random effects included location (transect nested within region) and date (year). Random effects that did not significantly explain variation were not included. Statistics are reported comparing nested models with and without land-use treatments through Akaike Information Criteria (AIC) and likelihood-ratio tests.

<b>Response Variable</b>	<b>Random Effects</b>	<b>Error Structure</b>	<b>ΔAIC</b>	<b>LRT (<math>\chi^2</math>)</b>	<b>P</b>
Phylogenetic diversity (PD; square transformed)	Transect+Year	Gaussian, identity link	-33.2	37.2	< 0.01
Deviation from expected PD	Region/Transect +Year	Gaussian, identity link	-25.3	31.3	<0.01
Residual PD (controlled for species richness)	Region/Transect	Gaussian, identity link	-25.3	35.5	<0.01
Raw species richness	Region/Transect	Poisson, log link	-20.5	24.5	< 0.01
Estimated richness (Chao)	Region/Transect	Poisson, log link	-20.9	24.9	< 0.01
Mean Phylogenetic Distance (MPD, global pool)	Region/Transect	Gaussian, identity link	-46.1	50.1	< 0.01
MPD (regional pool)	Transect	Gaussian, identity link	-50.1	55.0	< 0.01
MPD (land use pool)	Region/Transect	Gaussian, identity link	0.3	3.7	0.15
MPD (regional/land use pool)	Transect	Gaussian, identity link	3.0	1.0	0.61
Mean Nearest Taxon Distance (MNTD, global pool)	Region/Transect	Gaussian, identity link	-22.8	26.8	< 0.01
MNTD (regional pool)	Transect	Gaussian, identity link	-19.8	23.8	< 0.01
MNTD (land use pool)	Region/Transect	Gaussian, identity link	-8.3	12.3	< 0.01
MNTD (regional/land use pool)	Transect	Gaussian, identity link	-2.7	6.7	0.03
Evolution Distinctiveness (ED, Fair Proportion)	Region/Transect	Gaussian, identity link	-7.3	11.3	<0.01
ED (Exclude highest ED spp.)	Transect	Gaussian, identity link	-34.6	38.6	<0.01
Diversification Rate (DR)	Transect	Gaussian, identity link	-30.5	34.5	<0.01
Diversifications (last 1 MYRs)	Transect	Poisson, log link	NA	No converg.	NA
Diversifications (last 2 MYRs)	Transect	Poisson, log link	NA	No converg.	NA
Diversifications (last 3 MYRs)	Transect	Poisson, log link	-29.6	33.6	< 0.01
Diversifications (last 4 MYRs)	Transect	Poisson, log link	-1.7	5.7	0.06
Diversifications (last 5 MYRs)	Transect	Poisson, log link	-7.4	11.4	< 0.01
Diversifications (last 6 MYRs)	Transect	Poisson, log link	-10.1	14.1	< 0.01
Diversifications (last 7 MYRs)	Transect	Poisson, log link	-18.3	22.3	< 0.01
Diversifications (last 8 MYRs)	Transect	Poisson, log link	-20.9	24.9	< 0.01
Diversifications (last 9 MYRs)	Transect+Year	Poisson, log link	-18.9	22.9	< 0.01
Diversifications (last 10 MYRs)	Transect+Year	Poisson, log link	-21.5	25.5	< 0.01



**Table S6:** Agriculture affiliated birds have higher diversification rates, and are associated with natural open habitats. Values are derived from PGLS models, modeling covariance of pairwise species residuals according to Brownian motion evolution with Pagel’s  $\lambda$  transformation. For diversification rate (DR) versus Habitat Affinity Indices, values in cells represent slopes (*i.e.* how much average habitat affinity is expected to change as a result of increasing DR by 1). For natural open habitats versus Habitat Affinity Indices, values can be interpreted as mean differences in habitat affinities between species that are found in natural open habitats and those that are not. For comparisons of DR versus use of natural open habitats, values can be interpreted as mean differences in DR between species that are found in natural open habitats and those that are not. Positive values (grey backgrounds) indicate positive correlation between a habitat affinity and DR or use of natural open habitats. Negative values (red backgrounds) indicate negative correlation between affinity for a particular habitat and DR, or use of natural habitat type. Note that the habitat affinity indices take into account mean occupancy across land-use types, so should be read as relative preference for a land-use over the two other land-uses. All values are the median parameter estimates across 500 trees. Asterisks indicate level of significance from median likelihood ratio tests across 500 trees (\*  $p < 0.05$ , \*\*  $p < 0.01$ , \*\*\*  $p < 0.001$ ). In parentheses, we also provide the proportion of models across the 500 trees for which  $p < 0.05$ . Finally, the median value of Pagel’s  $\lambda$  estimated from all 500 trees is provided below slope estimates.

Habitat Affinity Index		Season	DR (versus Hab. Aff. Indices)	Natural Open Habitat				
				Along Waterways	Clearings	Savanna	Scrub & Brush	Forest Gaps
Forest	Dry	-1.92* (1.0) $\lambda = 0.48$	-0.85*** (1.0) $\lambda = 0.43$	0.06 (0.0) $\lambda = 0.48$	-1.04*** (1.0) $\lambda = 0.41$	-0.34 (0.0) $\lambda = 0.45$	1.09** (1.0) $\lambda = 0.44$	
	Wet	-2.20** (1.0) $\lambda = 0.39$	-0.75** (1.0) $\lambda = 0.35$	0.19 (0.0) $\lambda = 0.40$	-1.04*** (1.0) $\lambda = 0.32$	-0.50* (0.89) $\lambda = 0.35$	1.07** (1.0) $\lambda = 0.35$	
Diversified Agriculture	Dry	1.60** (1.0) $\lambda = 0.38$	0.39** (1.0) $\lambda = 0.36$	0.04 (0.0) $\lambda = 0.37$	0.41 (0.0) $\lambda = 0.35$	0.28 (0.01) $\lambda = 0.36$	-0.59** (1.0) $\lambda = 0.36$	
	Wet	1.95** (1.0) $\lambda = 0.26$	0.30* (1.0) $\lambda = 0.25$	0.01 (0.0) $\lambda = 0.25$	0.26* (1.0) $\lambda = 0.24$	0.39** (1.0) $\lambda = 0.23$	-0.59** (1.0) $\lambda = 0.25$	
Intensive Monocultures	Dry	0.28 (0.0) $\lambda = 0.45$	0.47*** (1.0) $\lambda = 0.38$	-0.08 (0.0) $\lambda = 0.45$	0.66*** (1.0) $\lambda = 0.37$	0.07 (0.0) $\lambda = 0.43$	-0.52** (1.0) $\lambda = 0.40$	
	Wet	0.25 (0.0) $\lambda = 0.34$	0.46*** (1.0) $\lambda = 0.28$	-0.16 (0.0) $\lambda = 0.35$	0.81*** (1.0) $\lambda = 0.27$	0.12 (0.0) $\lambda = 0.31$	-0.50* (1.0) $\lambda = 0.30$	
			<b>DR (versus Nat. Open Hab.)</b>	-0.03 (0.0) $\lambda = 0.84$	0.02 (0.0) $\lambda = 0.84$	0.05* (0.99) $\lambda = 0.84$	-0.03* (0.68) $\lambda = 0.87$	-0.01 (0.0) $\lambda = 0.84$

## References and Notes

1. D. S. Karp, A. J. Rominger, J. Zook, J. Ranganathan, P. R. Ehrlich, G. C. Daily, Intensive agriculture erodes  $\beta$ -diversity at large scales. *Ecol. Lett.* **15**, 963–970 (2012). [Medline doi:10.1111/j.1461-0248.2012.01815.x](#)
2. I. Perfecto, J. H. Vandermeer, A. Wright, *Nature's Matrix: Linking Agriculture, Conservation, and Food Sovereignty* (Cromwell, London, 2009).
3. C. Kremen, A. Miles, *Ecol. Soc.* **17**, 40 (2012).
4. M. L. McKinney, J. L. Lockwood, Biotic homogenization: A few winners replacing many losers in the next mass extinction. *Trends Ecol. Evol.* **14**, 450–453 (1999). [Medline doi:10.1016/S0169-5347\(99\)01679-1](#)
5. A. Purvis, P. M. Agapow, J. L. Gittleman, G. M. Mace, Nonrandom extinction and the loss of evolutionary history. *Science* **288**, 328–330 (2000). [Medline doi:10.1126/science.288.5464.328](#)
6. K. J. Gaston, T. M. Blackburn, Evolutionary age and risk of extinction in the global avifauna. *Evol. Ecol.* **11**, 557–565 (1997). [doi:10.1007/s10682-997-1511-4](#)
7. D. P. Faith, Conservation evaluation and phylogenetic diversity. *Biol. Conserv.* **61**, 1–10 (1992). [doi:10.1016/0006-3207\(92\)91201-3](#)
8. M. Winter, V. Devictor, O. Schweiger, Phylogenetic diversity and nature conservation: Where are we? *Trends Ecol. Evol.* **28**, 199–204 (2013). [Medline doi:10.1016/j.tree.2012.10.015](#)
9. G. M. Mace, J. L. Gittleman, A. Purvis, Preserving the tree of life. *Science* **300**, 1707–1709 (2003). [Medline doi:10.1126/science.1085510](#)
10. M. W. Cadotte, R. Dinnage, D. Tilman, Phylogenetic diversity promotes ecosystem stability. *Ecology* **93**, S223–S233 (2012). [doi:10.1890/11-0426.1](#)
11. M. W. Cadotte, Experimental evidence that evolutionarily diverse assemblages result in higher productivity. *Proc. Natl. Acad. Sci. U.S.A.* **110**, 8996–9000 (2013). [Medline doi:10.1073/pnas.1301685110](#)
12. R. Dinnage, M. W. Cadotte, N. M. Haddad, G. M. Crutsinger, D. Tilman, Diversity of plant evolutionary lineages promotes arthropod diversity. *Ecol. Lett.* **15**, 1308–1317 (2012). [Medline doi:10.1111/j.1461-0248.2012.01854.x](#)
13. C. G. Willis, B. Ruhfel, R. B. Primack, A. J. Miller-Rushing, C. C. Davis, Phylogenetic patterns of species loss in Thoreau's woods are driven by climate change. *Proc. Natl. Acad. Sci. U.S.A.* **105**, 17029–17033 (2008). [Medline doi:10.1073/pnas.0806446105](#)

14. R. Dinnage, Disturbance alters the phylogenetic composition and structure of plant communities in an old field system. *PLOS ONE* **4**, e7071 (2009). [Medline doi:10.1371/journal.pone.0007071](#)
15. M. R. Helmus, W. B. Keller, M. J. Paterson, N. D. Yan, C. H. Cannon, J. A. Rusak, Communities contain closely related species during ecosystem disturbance. *Ecol. Lett.* **13**, 162–174 (2010). [Medline doi:10.1111/j.1461-0248.2009.01411.x](#)
16. L. D. Verde Arregoitia, S. P. Blomberg, D. O. Fisher, Phylogenetic correlates of extinction risk in mammals: Species in older lineages are not at greater risk. *Proc. Biol. Sci.* **280**, 20131092 (2013). [Medline doi:10.1098/rspb.2013.1092](#)
17. W. Jetz, G. H. Thomas, J. B. Joy, D. W. Redding, K. Hartmann, A. O. Mooers, Global distribution and conservation of evolutionary distinctness in birds. *Curr. Biol.* **24**, 919–930 (2014). [Medline doi:10.1016/j.cub.2014.03.011](#)
18. W. Jetz, G. H. Thomas, J. B. Joy, K. Hartmann, A. O. Mooers, The global diversity of birds in space and time. *Nature* **491**, 444–448 (2012). [Medline doi:10.1038/nature11631](#)
19. Materials and methods are available as supplementary materials on *Science* Online.
20. S. P. Blomberg, T. Garland Jr., A. R. Ives, Testing for phylogenetic signal in comparative data: Behavioral traits are more labile. *Evolution* **57**, 717–745 (2003). [Medline doi:10.1111/j.0014-3820.2003.tb00285.x](#)
21. M. Pagel, Inferring the historical patterns of biological evolution. *Nature* **401**, 877–884 (1999). [Medline doi:10.1038/44766](#)
22. J. A. Royle, M. Kéry, A Bayesian state-space formulation of dynamic occupancy models. *Ecology* **88**, 1813–1823 (2007). [Medline doi:10.1890/06-0669.1](#)
23. S. G. Driese, K. H. Orvis, S. P. Horn, Z. H. Li, D. S. Jennings, Paleosol evidence for Quaternary uplift and for climate and ecosystem changes in the Cordillera de Talamanca, Costa Rica. *Palaeogeogr. Palaeoclimatol. Palaeoecol.* **248**, 1–23 (2007). [doi:10.1016/j.palaeo.2006.11.013](#)
24. M. Irestedt, J. Fjeldså, L. Dalén, P. G. P. Ericson, Convergent evolution, habitat shifts and variable diversification rates in the ovenbird-woodcreeper family (Furnariidae). *BMC Evol. Biol.* **9**, 268 (2009). [Medline doi:10.1186/1471-2148-9-268](#)
25. J. T. Weir, D. Schluter, The latitudinal gradient in recent speciation and extinction rates of birds and mammals. *Science* **315**, 1574–1576 (2007). [Medline doi:10.1126/science.1135590](#)

26. D. S. Karp, G. Ziv, J. Zook, P. R. Ehrlich, G. C. Daily, Resilience and stability in bird guilds across tropical countryside. *Proc. Natl. Acad. Sci. U.S.A.* **108**, 21134–21139 (2011). [Medline doi:10.1073/pnas.1118276108](#)
27. R. Macarthur, R. Levins, The limiting similarity, convergence, and divergence of coexisting species. *Am. Nat.* **101**, 377–385 (1967). [doi:10.1086/282505](#)
28. G. W. Luck, S. Lavorel, S. McIntyre, K. Lumb, Improving the application of vertebrate trait-based frameworks to the study of ecosystem services. *J. Anim. Ecol.* **81**, 1065–1076 (2012). [Medline doi:10.1111/j.1365-2656.2012.01974.x](#)
29. C. O. Webb, Exploring the phylogenetic structure of ecological communities: An example for rain forest trees. *Am. Nat.* **156**, 145–155 (2000). [Medline doi:10.1086/303378](#)
30. G. Stiles, A. Skutch, *A Guide to the Birds of Costa Rica* (Cornell Univ. Press, Ithaca, NY, 1989).
31. J. A. Royle, R. M. Dorazio, *Hierarchical Modeling and Inference in Ecology* (Academic Press, London, 2008).